Virus Research 339 (2024) 199282

Contents lists available at ScienceDirect

Virus Research

journal homepage: www.elsevier.com/locate/virusres

DUSP1 mRNA modulation during porcine circovirus type 2 and porcine reproductive and respiratory syndrome virus co-infection regulates viruses replication

Yaima Burgher-Pulgaron [a], Chantale Provost [b], Fernando Alvarez [d], Europa Meza-Serrano [c], Marie-Jeanne Pesant [a], Christopher A. Price [c], Carl A. Gagnon [a,b,*]

[a] The Swine and Poultry Infectious Diseases Research Centre (CRIPA-FRQNT), Faculté de Médecine Vétérinaire (FMV), Université de Montréal, 3200 rue Sicotte, St-Hyacinthe, Québec, Canada, J2S 2M2
[b] Molecular Diagnostic Laboratory, Centre de Diagnostic Vétérinaire de l'Université de Montréal (CDVUM), FMV, Canada
[c] Centre de Recherche en Reproduction Animale, FMV, Université de Montréal, Canada
[d] Infectious Diseases and Immunity in Global Health (IDIGH), McGill University, 1001 Décarie, Montréal, Québec, Canada, H4A 3J1

ARTICLE INFO

Keywords:
PCV2b
PRRSV
Co-infection
NPTr-CD163 cells
DUSP1

ABSTRACT

The effects of porcine circovirus type 2b (PCV2b) and porcine reproductive and respiratory syndrome virus (PRRSV) co-infection in epithelial cells of the swine respiratory tract is unknown. In the present study, the newborn pig trachea cell line NPTr-CD163, which is permissive to both viruses, was persistently infected with PCV2b and then with PRRSV. Viral replication, cell viability, cytokines' mRNA expression, and modulation of cellular genes expression were evaluated in infected cells. In NPTr-CD163 co-infection model, PCV2b replication was enhanced while PRRSV replication was suppressed. Cell viability was significantly decreased during PCV2b single infection and co-infection compared to mock-infected and PRRSV single infected cells. However, no difference was observed in cell viability between PCV2b and PCV2b/PRRSV infected cells. The *IL6, IL8* and *IL10* mRNA expression was significantly higher in co-infected cells compared to PCV2b and PRRSV single infected cells. Moreover, the *IFN-α/β* expression was significantly reduced in co-infected cells compared to PCV2b infected cells whereas it remained higher compared to PRRSV infected cells. The differential gene expression analysis revealed that the mRNA expression level of the cellular gene *DUSP1* was significantly higher in all PRRSV infection models compared to PCV2b single infected cells. Knockdown of *DUSP1* expression in co-infected cells significantly reduced PCV2b replication, suggesting a role for *DUSP1* in PCV2b/PRRSV pathogenesis.

1. Introduction

Swine respiratory diseases have a huge impact on this industry (Brockmeier et al., 2002). One of the issues that make it difficult to control respiratory problems on pig farms is that they frequently involve the association of multiple agents, a phenomenon known as porcine respiratory disease complex (PRDC). Porcine circovirus type 2 (PCV2) and porcine reproductive and respiratory syndrome virus (PRRSV) are two important viral pathogens which are part of the PRDC (Brockmeier et al., 2002; Opriessnig et al., 2011).

PCV2 is a member of the *Circoviridae* viral family, genus *Circovirus* (Lefkowitz et al., 2018), with a small circular single-stranded DNA genome (Lefkowitz et al., 2017). Eight genotypes of PCV2 have been described so far (PCV2a-PCV2h) (Franzo and Segales 2018; Wang et al., 2020; Link et al., 2021). PCV2 is associated with several syndromes and pathological conditions in pigs, which have been grouped under the term porcine circovirus-associated diseases (PCVAD) (Gillespie et al., 2009). PCVAD includes the post-weaning multisystemic wasting syndrome (PMWS), porcine dermatitis and nephropathy syndrome (PDNS), reproductive failure, PRDC, granulomatous enteritis, necrotizing lymphadenitis, and exudative epidermitis (Allan et al., 2000a; Thomson et al., 2000; Pallares et al., 2002; Dan et al., 2003; Kim et al., 2003; Gillespie et al., 2009). It is reported that co-infection of PCV2 with other swine pathogens may enhance PCV2 infection and the severity of PCVAD (Dorr et al., 2007; Gillespie et al., 2009; Yi and Liu 2010; Opriessnig and Halbur 2012; Hu et al., 2017).

* Corresponding author at: Faculté de Médecine Vétérinaire, 3200 rue Sicotte, office 3963, Saint-Hyacinthe, Québec, Canada, J2S 2M2.
E-mail address: carl.a.gagnon@umontreal.ca (C.A. Gagnon).

https://doi.org/10.1016/j.virusres.2023.199282
Received 2 August 2023; Received in revised form 18 November 2023; Accepted 20 November 2023

PRRSV is the etiological agent of the porcine reproductive and respiratory syndrome (PRRS), which is considered as one of the most economical important disease in swine production (Neumann et al., 2005). PRRSV is an enveloped, single-stranded positive sense RNA virus classified in the order *Nidovirales*, family *Arteriviridae.* It belongs to the genus *Betaarterivirus* that is divided into the species *Betaarterivirus suid 1* (formerly the European genotype or type I represented by the Lelystad strain) and *Betaarterivirus suid 2* (formerly the North American genotype or type II represented by the ATCC VR-2332 strain) (Lefkowitz et al., 2017). Along with respiratory and reproductive problems caused by PRRSV infection in pigs, reduced weight gain and an increase in mortality from secondary infections can also be observed (Solano et al., 1997; Thanawongnuwech et al., 2000a; Yu et al., 2012).

PCV2b and PRRSV have a worldwide distribution and co-infection with both viruses is reported as one of the most predominant pathogen combinations being involved in PMWS (Pallares et al., 2002; Gagnon et al., 2007) with a ratio of co-infection ranging from 20 % to 83 % (Sorden et al., 1998; Allan and Ellis 2000; Segales et al., 2002; Wellenberg et al., 2004). In fact, PRRSV infection is considered a major risk factor for PMWS in PCV2-infected pigs (Fraile et al., 2009). Moreover, several studies suggested that PRRSV may enhance PCV2 infection and the severity of PCVAD (Shi et al., 2008; Sinha et al., 2011; Opriessnig et al., 2012; Fan et al., 2013; Park et al., 2014).

PCV2 and PRRSV are transmitted through the oronasal route. Alveolar and/or intravascular macrophages are known as the major target cells for both PCV2 and PRRSV in the lungs (Thanawongnuwech et al., 2000b; Chang et al., 2005; Tsai et al., 2012). It has been reported that *in vitro* effects of PCV2/PRRSV co-infection in alveolar macrophages include a reduction in PRRSV antigen-containing rate and cytopathic effect, as well as an increase in the levels of *IL8, TNF-α, IFN-α*, and *FasL* transcripts (Tsai et al., 2012). Moreover, Miller et al. (2020) compared the transcriptome response within the tracheobronchial lymph nodes of swine experimentally infected with PCV2, PRRSV or influenza virus. The authors of the mentioned study identified differentially expressed genes (DEGs) and cellular pathways that were modulated by both, PCV2b and PRRSV infections. However, the samples for that study were obtained from single-infected animals and not from co-infected animals (Miller et al., 2020).

Respiratory epithelial cells are in the first line of defense against viruses infecting the respiratory tract. They have an important role in the initial recognition of viral pathogens via pattern recognition receptors (PRRs) and subsequent production of cytokines and chemokines to trigger innate and adaptive immune responses (Vareille et al., 2011; Günther and Seyfert 2018). Interestingly, PCV2 and/or PRRSV antigens have been observed in epithelial pulmonary cell types such as bronchiolar epithelial cells, sloughed pneumocytes, including some syncytial cells and epithelial cells of the lung parenchyma (Pol et al., 1991; Halbur et al., 1994; Rossow et al., 1996; Sirinarumitr et al., 2001). The effects of PCV2b/PRRSV co-infection have been widely studied in porcine primary alveolar macrophages (PAM) (Chang et al., 2005; Tsai et al., 2012). Nevertheless, to our knowledge, no study has been conducted to elucidate the *in vitro* effects of PCV2b/PRRSV co-infection in lung epithelial cells. The hypothesis of the present study is that PCV2b/PRRSV co-infection modify the pathogenesis of both viruses in porcine respiratory epithelial cells compared to PCV2b or PRRSV single-infected cells. In that regard, this research aimed to determine the effects of PCV2b/PRRSV co-infection on viral replication, cytokines transcriptional expression, cell viability and cellular gene expression using an *in vitro* porcine respiratory tract epithelial cells model. Comparative analysis of differential gene expression after 3′ mRNA-sequencing on single-infected and co-infected cells was carried out to identify DEGs that could be involved in the pathogenesis of PCV2b/PRRSV co-infection. Dual specificity phosphatase 1 gene (*DUSP1*) was identified among the DEGs in single-infected and co-infected cells. *DUSP1* has been previously implicated in the infection of several virus including Vaccinia virus (VACV) (Cáceres et al., 2013), JC polyomavirus (JCPyV) (Wilczek et al., 2021), Hepatitis C virus (HCV) (Choi et al., 2015), Human respiratory syncytial virus (RSV) (Robitaille et al., 2017), Sendai virus (SeV) (Robitaille et al., 2017) and SARS-CoV-2 virus (Goel et al., 2021), leading to either enhanced or reduced viral infection. In the present study, RNA interference (RNAi) methodology was used to confirm the role of *DUSP1* in viral replication during PCV2b/PRRSV co-infection.

2. Material and methods

2.1. Cell lines and viruses

The NPTr-CD163 cells, which were previously obtained (Provost et al., 2017), were cultured in Minimum Essential Medium (MEM) (Invitrogen Corporation, GibcoBRL, ON, Canada) supplemented with 10 % fetal bovine serum (FBS) (Wisent Bioproducts, QC, Canada), 1 mM sodium pyruvate, 10 I.U./mL of penicillin, 10 μg/mL of streptomycin and 250 g/L amphotericin B solution (Wisent Bioproducts, QC, Canada), as previously described (Burgher Pulgaron et al., 2023). MARC-145 cells (ATCC CRL-12,231) were maintained as previously described (Lévesque et al., 2014). All cell lines were cultivated at 37 °C in 5 % CO_2 atmosphere. The PCV2b strain (FMV-06–0732) used in this study was isolated from a 2006 Canadian PMWS clinical case (GenBank accession number: JQ994270). The virus was propagated into NPTr-CD163 cells, purified and concentrated following ultracentrifugation on a 30 % sucrose cushion using the SW28 Beckman Coulter rotor (Beckman Coulter Canada Inc., Mississauga, ON, Canada) at 25,000 rpm for 4 h. The PRRSV type II Quebec reference strain IAF-Klop, previously isolated in Canada (Dea et al., 1996), was used in this study. The virus was propagated in MARC-145 cell line as previously described (Provost et al., 2012). The PCV2b and PRRSV infectious viral titers were determined in NPTr-CD163 and MARC-145 cells, respectively, by the Spearman-Kärber method (Spearman, 1909; Kärber, 1931). Immunofluorescence assay (IFA) was used to identify PCV2b antigens expressing cells whereas cytopathic effect (CPE) was used for PRRSV. The viral titer was expressed in tissue culture infectious dose 50 % per mL ($TCID_{50}$/mL).

2.2. PCV2b and PRRSV co-infection

NPTr-CD163 cells (6×10^6 cells) were infected in suspension with PCV2b (MOI 0.05) and at least three passages were done with the infected cells to achieve a continuous viral infection. Then, PCV2b-infected cells were co-infected with PRRSV at 0.5 MOI for 4 h and washed three times with phosphate-buffered saline (PBS) 1X. Fresh medium with 2 % FBS was added and the cells were incubated for 24 h.

2.3. Immunofluorescence assay

An immunofluorescence assay (IFA) was used to confirm if PCV2b and PRRSV dual infection occurred in NPTr-CD163 cells. Briefly, 1×10^4 PCV2b/PRRSV co-infected cells were fixed with a mixture of acetone-methanol (50/50, v/v) and incubated for 20 min at room temperature. Then, cells were washed three times with PBS 1X and were permeabilized with a solution containing 0.1 % triton X-100 in PBS for 10 min. Following incubation with a blocking solution (1 % bovine serum in PBS-Tween 20 for 20 min) the cells were incubated with a 1/200 dilution of a polyclonal PCV2 porcine antiserum and a 1/200 dilution of α7 rabbit monospecific antisera, a specific anti-N PRRSV antibody (Gagnon et al., 2003). After three PBS 1X washes, cells were incubated with a 1/75 dilution of a goat anti-swine rhodamine conjugated antibody (Jackson ImmunoResearch, PA, USA) and a 1/200 dilution of goat anti-rabbit FITC conjugated (Invitrogen, CA, USA). After three washing steps, the cells were visualized using a DMI 4000B reverse fluorescence microscope. Photographs of the cells were taken with a DFC 490 digital camera and the images were analyzed using the Leica Application Suite Software, version 2.4.0 (Leica Microsystems Inc., Richmond Hill,

Canada).

2.4. PCV2b and PRRSV genome copy number quantification

To quantify PCV2b in the infected cells, the latter were subjected to 3 rounds of freeze-thaw cycles to release the virus particles and the cell debris was removed by centrifugation at 8000 rpm at 4 °C for 15 min. Afterwards, 50 µL of sample were diluted in 150 µL of sterile PBS and treated with 20 µL of proteinase K (Qiagen™, Missisauga, ON, Canada) at 70 °C for 5 min. The DNA was purified with Qiagen's QIAamp DNA Mini Kit (Qiagen™, Missisauga, ON, Canada) according to the manufacturer instructions. Two microliters of purified DNA were used for qPCR reactions with Taq Man Fast Advanced Master Mix and a QuantStudio3 Real Time PCR System (Thermo Scientific). The primers and probes used for PCV2b quantification are shown in Supplemental Table S1. PCV2b genome copy number was determined by comparing sample results to a standard curve generated with ten-fold serially dilutions of PCV2b genomic DNA of known concentration. To establish the standard curve, the viral genome was extracted with Qiagen's QIAamp DNA Mini Kit (Qiagen™, Missisauga, ON, Canada) from the purified viral stock. The DNA concentration was measured using a Qubit Fluorometer (Thermo Fisher, Walthman, MA, USA). The nanograms of purified genomic DNA was converted to copy number using a free-access copy number calculator (sciprim.com/html/copyNumb.v2.0.html).

For PRRSV quantification, total RNA was extracted from infected cells using the RNeasy Mini Kit (Qiagen) and quantified as described above. The purified RNA (1 µg) was used in real-time RT-PCR reactions using the TaqMan Fast Virus 1-Step Master Mix (Thermo Fisher) and a QuantStudio3 Real Time PCR apparatus (Thermo Fisher Scientific). The instrument's software determined the normalized quantity of PRRSV in the samples using standard curves for PRRSV and the endogenous controls (β_2-microglobulin (*B2M*), β-actin (*ACTB*) and peptidylprolyl isomerase A (*PPIA*)). To generate standard curves of the endogenous control genes, total RNA was extracted and quantified from mock-infected cells as described above and ten-fold serial dilutions were done. The software generated the standard curves for each endogenous control gene from the same RNA preparations using the corresponding primers and probes (Supplemental Table S1). To generate the standard curve used to interpolate PRRSV genome copy number in the samples, PRRSV genome was purified using RNeasy Mini Kit (Qiagen) from highly purified viral stock. Thereafter, it was quantified using a Qubit Fluorometer (Thermo Fisher, Walthman, MA, USA). and converted to copy number using the free-access copy number calculator described above. Finally, ten-fold serial dilutions were done as described above. The primers and probes used for PRRSV quantification are shown in Supplemental Table S1.

2.5. Viral replication kinetics

1×10^5 NPTr-CD163 cells were infected with PCV2b and/or PRRSV as described above. Cells were collected at 4, 24, 48, 72 and 96 h PRRSV post-infection and each virus was quantified by qPCR as described above. All viral infections were performed two times in triplicate.

2.6. Cell viability assay

Cell viability assay was performed on 10^4 mock-infected, single-infected and co-infected cells at 72 h post-infection (hpi) using the Cell titer 96 Aqueous One Solution Cell Proliferation Assay kit (Promega, Madison, WI, USA), following the manufacturer's instructions. After adding 20 µL of the reagent to each well, the cells were incubated for 2 h at 37 °C and the absorbance was measured at 490 nm (Biotek® Synergy HT plate reader, Vermont, USA). The percentage of cell viability was calculated using the mock-infected cells as control. Each experiment was performed in triplicate and repeated at least two times.

2.7. Cytokine mRNAs' expression

The mRNA expression levels of *IL6, IL8, IL10, IFN-α, IFN-β* and *IFN- γ* in PCV2b/PRRSV single-infected and co-infected cells were measured by RT-qPCR. For that purpose, 6×10^6 infected and mock-infected cells were incubated in 6 well plates for 72 h. Total cellular RNA was extracted and purified using the RNeasy Mini Kit (Qiagen), according to the manufacturer's instructions. The RNA concentration was measured with a Qubit fluorometer (Thermo Fisher, Walthman, MA, USA) and 1 µg of purified RNA was reverse transcribed with M-MLV reverse transcriptase (Invitrogen, Burlington, ON, CA), following the manufacturer's protocol. The cDNA was then amplified with PowerTrack SYBR Green Master Mix kit (Thermo Fisher, Walthman, MA, USA) with a QuantStudio 3 Real-Time PCR System (Thermo Fisher, Walthman, MA, USA). The $2^{-\Delta\Delta Ct}$ method was used to quantify the differences between groups. Normalized genes *B2M, ACTB* and *PPIA* were used to compensate for potential differences in cDNA amounts. Mock-infected cells were used as a calibrator reference in the analysis. The primers used in this assay are described in Supplemental Table S1.

2.8. 3′ RNA-seq transcriptome library preparation and sequencing

Total cellular RNA was purified from 1×10^6 single infected, co-infected or mock-infected cells at 72 hpi using the RNeasy Mini Kit (Qiagen, Valencia, CA, USA), according to the manufacturer's instructions. Before library construction, RNA concentration and quality were assessed with Agilent 2100 Bioanalyzer using RNA 6000 Nano kit (Agilent Technologies, CA, USA). Only extracted/purified RNAs with an RNA integrity number (RIN) of at least 7 were used for the mRNA libraries synthesis. A total of 0.5 ng of purified RNA was used for the mRNA library constructions with the QIAseq UPX 3′ Transcriptome Kit (Qiagen, Toronto, ON, Canada), according to the manufacturer's protocol. Briefly, using this kit, each RNA molecule in the samples is tagged with a Unique Molecular Index (UMI) and an unique sample ID during reverse transcription, so all individually tagged cDNAs from all samples can be combined, which enables all subsequent library construction steps to be performed in a single tube (https://www.qiagen.com). After reverse transcription reactions, the synthesized cDNAs from PCV2b-, PRRSV-, PCV2b/PRRSV- and mock-infected cells were combined in a single tube to obtain the sequencing libraries according to the QIAseq UPX 3′ Transcriptome Kit (Qiagen) protocol. Libraries concentrations were measured with a Qubit Fluorometer (Thermo Fisher, Walthman, MA, USA) and their quality were assessed using the Agilent 2100 Bioanalyzer instrument with the Agilent High Sensitivity DNA kit (Agilent Technologies, CA, USA). High throughput sequencing was carried out using the MiSeq sequencing platform (Illumina, CA, USA). The libraries were sequenced using v3 (150-cycles) MiSeq Reagent Kits from Illumina.

2.9. Identification of differentially expressed genes

The sequencing raw data were imported in FASTQ format into CLC Genomics Workbench software (QIAGEN, version 22.0.1, Qiagen, CA, USA). The reads were demultiplexed using the UPX 3′ RNA application, quantified with the Quantify QIAseq UPX 3′ ready-to-use workflow and the generated gene expression annotations obtained after mapping to the reference genome (Sscrofa11.1) were used in subsequent data analyses. The differential expression analysis was performed with the Differential Expression for RNA-Seq tool available in CLC Genomics Workbench software, version 20.0. Here, a per-sample library size normalization is automatically performed using the TMM (trimmed mean of M values) normalization method (Oshlack et al., 2010; Robinson and Oshlack, 2010) in order to compensate for differences in the sequencing depth between samples. The gene expression levels of PCV2b-, PRRSV- and PCV2b/PRRSV- infected cells were compared to the one found in mock-infected control cells. A False Discovery Rate

(FDR) <0.05 and a fold-change cutoff of 1.5 was used to identify significant differentially expressed genes (DEGs). Physical interactions between the identified DEGs in each type of infection were determined with Metascape (Zhou et al., 2019).

2.10. GO and KEGG enrichment analysis

Gene Ontology (biological process) enrichment analysis was performed with PANTHER (Ashburner et al., 2000; The-Gene-Ontology--Consortium 2021). An FDR < 0.05 was used to filter the over-represented or enriched terms from the analyzed DEG sets. In order to remove redundant gene ontology (GO) terms, the terms presenting a Fold Enrichment > 2 were imported into REVIGO (Supek et al., 2011). The terms having dispensability values score < 0.4 were retained. An enrichment analysis of the KEGG cell pathways was performed using the Database for Annotation, Visualization and Integrated Discovery (DAVID, 2021) (Huang et al., 2009). Significant enriched pathways in the analyzed DEG sets were filtered using an FDR cut-off < 0.05 and Fold Enrichment > 2.

2.11. DUSP1 gene knockdown in PCV2b/PRRSV co-infected cells

Prior to *DUSP1* knockdown experiment, *DUSP1* mRNA fold regulation was determined in PCV2b and PRRSV single-infected and co-infected cells at 24, 48, 72 and 96 hpi. *DUSP1* mRNA expression levels were measured by RT-qPCR using *DUSP1* specific primers (Supplemental Table S1) and the same protocol described above for cytokine mRNA expression analysis. Thereafter, the *DUSP1* expression was reduced using the dicer-substrate short interfering RNAs (DsiRNAs) molecules. Four DsiRNAs targeting porcine *DUSP1* were generated using the DsiRNA design tool from Integrated DNA Technologies (Integrated DNA Technologies, IDT, CA USA). DsiRNAs are chemically synthesized 25/27-mer duplex RNAs that have increased potency compared to 21mer siRNAs (Integrated DNA Technologies, IDT, CA USA). *DUSP1* specific DsiRNAs and scrambled DsiRNA negative control (Integrated DNA Technologies, IDT, CA USA) were resuspended in RNase-free Duplex Buffer (Integrated DNA Technologies, IDT, CA USA) according to IDT Technologies guidelines. The performance of all four designed DsiRNAs was initially evaluated in mock-infected cells. To accomplish this objective, reduced expression of *DUSP1* mRNA and cell viability were determined in DsiRNAs transfected mock cells. DsiRNA # 10 and DsiRNA # 12 were selected for further evaluations and transfection experiments in co-infected cells. The sequences of DsiRNA #10 and #12 are shown in Supplemental Table S1 and the effect of DsiRNA # 10, DsiRNA # 12 or a mix of both DsiRNAs on DUSP1 mRNA expression and viral replication is showed in Supplemental Fig. S1 and Fig. 8.

Reverse transfection experiments were performed using Lipofectamine RNAiMAX reagent (Invitrogen by Life Technologies) diluted in Opti-MEM Medium, according to the manufacturer's instructions. DsiRNA #10 and DsiRNA #12 were pooled and diluted in Opti-MEM Medium. Then, DsiRNA-RNAiMAX complexes were prepared in a 24-well plate (1:1 ratio) with DsiRNAs at a final concentration of 10 nM. PCV2b-previously infected cells (1×10^5 cells) were added to DsiRNA-RNAiMAX complexes in each well, allowing the cells to growth for 24 h before PRRSV infection. Following PRRSV infection, transfected and co-infected cells were incubated for 3 days at 37 °C and then, viral replication was determined and cells were processed to quantify *DUSP1* mRNA and protein expressions. Reverse transfection experiments using scrambled DsiRNA negative control (Integrated DNA Technologies, IDT, CA USA) were performed in parallel as described above. A minimum of three biological replicates were done.

2.12. Western blot assays

Cells were disrupted in Laemmli buffer (62.5 mM Tris (pH 6.8), 2 % SDS, 10 % glycerol and 100 mM DTT) 72 h after cell infections or transfection assay. Briefly, the cells were washed in the plate three times with ice-cold PBS 1X. After adding cold Laemmli sample buffer, the cells were scraped, collected and the samples were boiled at 100 °C for 5 min. Following a centrifugation step at 14 000 rpm for 5 min at 4 °C, the supernatant was collected and stored at −80 °C until further use. Total cell protein concentrations was measured using a Qubit Fluorometer (Thermo Fisher, Walthman, MA, USA), following the manufacturer's instructions. Using a Tetra cell apparatus (Bio-rad), 20 µg of total proteins were resolved in 12 % SDS-PAGE. Proteins were then transferred into a LF-PVDF membranes using a tank blotting system (TransBlot; BioRad, Mississauga, ON, Canada) and membranes were subsequently cut to horizontal strips corresponding to the expected kilodaltons (kDa) molecular weight of targeted proteins. The membranes were blocked in TTBS (tris-buffered saline with 0.1 % Tween 20) containing 5 % (w/v) BSA and incubated with anti-DUSP1 (1/2000 in TTBS, Biorbyt, orb317657, Invitrogen). Anti-mouse horseradish peroxidase-conjugated (Cell Signaling Technology, USA) diluted 1/20,000 in TTBS containing 5 % (w/v) BSA was used as the secondary antibody. Each incubation step was followed by three washes of 5 min each in TTBS (10 mM Tris–HCl, 150 mM NaCl, and 0.1 % (v/v) Tween-20, pH 7.5). The protein bands were visualized using ECL detection kits (Bio-rad). The same membranes were mild striped and were re-probed with anti-β-actin (1/10,000 in TTBS; sc-47,778 HRP Santa Cruz) to confirm equal protein loading into the electrophoretic polyacrylamide gel. Densitometric analyses were performed with ImageJ software after background subtraction. For each protein, intensities were calibrated to a calibrator sample, and the calibrated intensity was normalized compared to β-actin control.

2.13. Statistical analyses

All statistical analyses were performed using GraphPad Prism software (GraphPad Prism 7.0.0). The different statistical tests being used within each analysis are described in figure legends. Data are presented as means ± standard deviation (SD) from at least three independent experiments. Experimental groups were considered significantly different when p-value < 0.05.

3. Results

3.1. NPTr-CD163 cells, a new model for PCV2b/PRRSV co-infection studies

NPTr-CD163 cells were infected with PCV2b virus for 2–3 passages to obtain persistently infected cells and then were co-infected with PRRSV for 96 h. This approach allowed to study the cells co-infected with PCV2b and PRRSV even when both viruses have different replication kinetics. Moreover, this strategy resembles the dynamics of viral mixed infections in the field where subclinical PCV2b infections are widespread and animals may be infected with PCV2b before being infected with PRRSV. IFA results showed that NPTr-CD163 cells could support a stable PCV2b infection. Interestingly, with IFA it was evidenced that both PCV2b and PRRSV viruses can co-localize simultaneously in the same NPTr-CD163 infected cells (Fig. 1D).

However, during PCV2b/PRRSV co-infection, most of the cells were infected only by one of the virus (Fig. 1D). Sirinarumitr et al. (2001) reported similar results using double *in situ* hybridization of pigs lungs infected by both PCV/PRRSV viruses (Sirinarumitr et al., 2001). Thus, our model recapitulates key observations that PCV2 and PRRSV can co-localize in swine respiratory cells.

3.2. PCV2b and PRRSV dual infection modulates viral replication kinetics in NPTr-CD163 cells

To study the effect of PCV2b and PRRSV dual infection on viral replication, the replication efficiency of each virus was determined in the co-infection model compared to single-infected cells. PCV2b

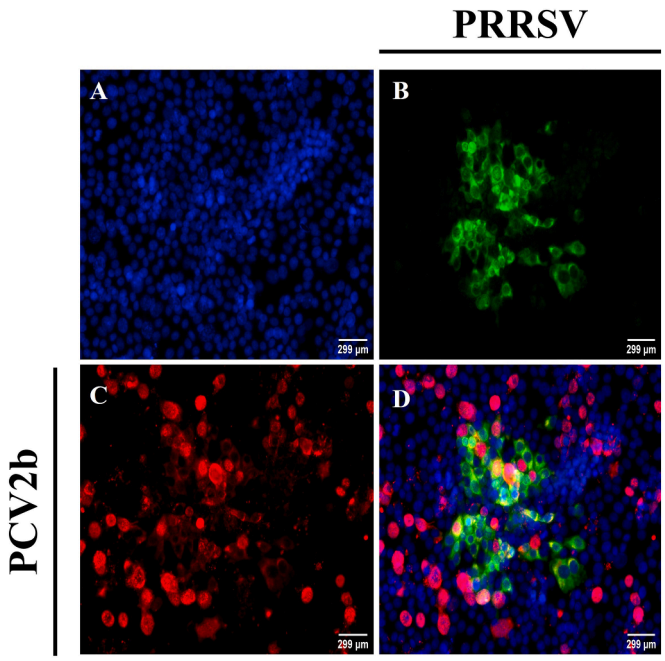

Fig. 1. PCV2b and PRRSV can infect and co-localize in NPTr-CD163 cells. IFA was performed on PCV2b (red) and PRRSV (green) co-infected cells at 72 hpi. The cells were infected with 0.05 MOI of PCV2b and passaged at least three times. Then, PCV2b-infected cells were infected with 0.5 MOI of PRRSV. Nuclear staining with DAPI is shown in blue. Co-localization pictures were done with ImageJ. Mock-, PRRSV-, PCV2b- and PCV2b/PRRSV infected cells are shown in Fig. 1A, 1B, 1C and 1D, respectively.

replication was found to significantly increase starting at 48 hpi in co-infected cells compared to PCV2b single-infected cells (Fig. 2A), whereas PRRSV replication was significantly decreased at 72 hpi and 96 hpi in co-infected cells compared to PRRSV single-infected cells (Fig. 2B). These results highlight that the replication machinery of this respiratory cell line may be hijacked by the co-infection.

3.3. PCV2b/PRRSV co-infection decreases cell viability in regards to PRRSV-single-infected cells

To determine the effect of PCV2b/PRRSV co-infection on cell viability, single-infected and co-infected cells were evaluated at 72 hpi. PRRSV infection alone did not affect NPTr-CD163 cell viability whereas PCV2b alone and in co-infection reduced the cell viability compared to the mock-infected cells (Fig. 3).

However, no difference was observed between co-infected and PCV2b single-infected cells suggesting that the effect on cell viability decrease is mostly driven by PCV2b. Collectively, these results reveal that PCV2b, but not PRRSV, could promote respiratory cell injury contributing to the pathogenesis of the co-infection *in vitro*.

3.4. Cytokines mRNA expression modulation in PCV2b/Prrsv co-infected cells

It is well known that PCV2b and PRRSV infections can alter the host immune response by modulating the expression of interleukins and interferons (Kekarainen et al., 2010; Sang et al., 2011). In the present study, *IL6, IL8, IL10, IFN-α, IFN-β* and *IFN-γ* mRNA expressions were up-regulated in PCV2b- and PCV2b/PRRSV- infected cells compared to mock-infected cells (fold change > 2) while PRRSV significantly increased the transcriptional expression of *IL8, IL10* and *IFN-γ* in

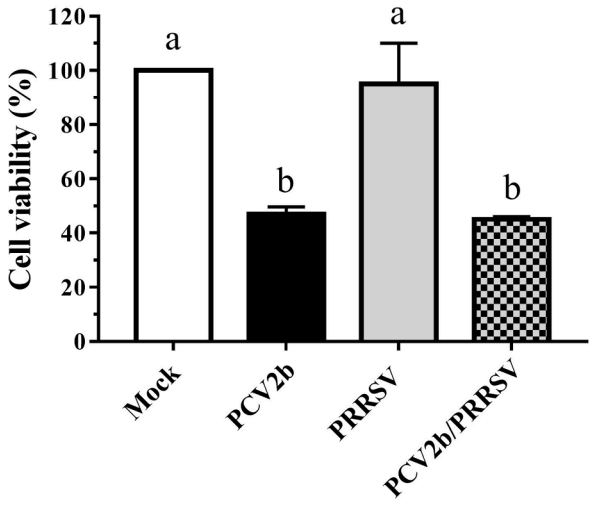

Fig. 3. PCV2b and PRRSV decrease cell viability in co-infected and PCV2b single-infected cells. Cell viability was determined at 72 hpi on mock-infected, single-infected or co-infected PCV2b/PRRSV cells. The data represents the percentage of cell viability in infected cells with respect to mock-infected cells and are presented with standard deviation (SD) of three biological replicates. Statistical analyses were done using one-way ANOVA followed by Tukey's multiple comparisons test. Bars labelled with different superscripts letters within the same assay indicates that these sets of data are statistically different ($p < 0.05$).

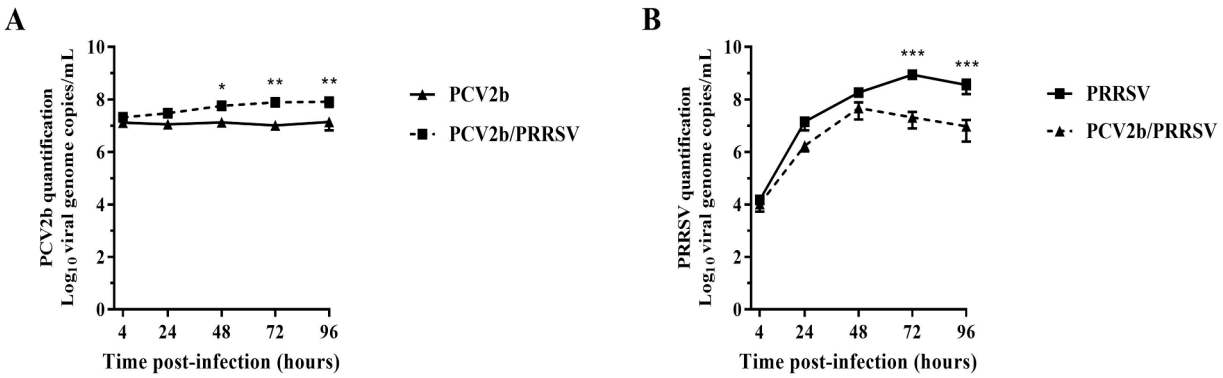

Fig. 2. PCV2b/PRRSV co-infection modulates viral replication in NPTr-CD163 cells. The PCV2b (A) and the PRRSV (B) genome copy number was measured in single infected and co-infected cells by qPCR and RT-qPCR, respectively. Statistical analyses were done using a two-way repeated measures ANOVA followed by Sidak's multiple comparisons test to compare the quantity of viral genome between single infected and co-infected cells at different time points. A Tukey's multiple comparisons test was performed to determine the statistically significant differences between time points in a same infection. Data are presented with standard deviation (SD) of three biological replicates. ** $p < 0.01$, * $p < 0.05$.

infected cells (Fig. 4).

In co-infected cells, interleukins mRNA expressions were significantly higher than in single-infected cells (Fig. 4A). Interestingly, *IFN-α/β* expression was significantly lower in co-infected cells than in cells infected only with PCV2b (Fig. 4B). Nevertheless, the *IFN-α/β* mRNA expression remained significantly higher in co-infected cells than in PRRSV single-infected cells and mock-infected cells. This could explain the reduction in PRRSV replication observed in dually infected NPTr-CD163 cells in the present study, considering that type I interferons inhibit PRRSV replication (Brockmeier et al., 2017; Zhu et al., 2021). Collectively, these results confirm that co-infection with both PCV2b and PRRSV differentially modulates cytokine transcriptional response in NPTr-CD163 cells compared to single-infected cells.

3.5. Identification of differentially expressed genes and enrichment analysis

To better characterize the transcriptional landscape conferred by the co-infection, the cellular gene expression profile was analyzed in single-infected and co-infected cells. Differential gene expression analysis identified 127, 32 and 84 DEGs in PCV2b-, PRRSV- and PCV2b/PRRSV-infected cells, respectively, compared to mock-infected cells (Fig. 5A). The DEGs in each infection and the level of modulation are shown in Supplemental Tables S2 and S3. GO enrichment analysis performed with the corresponding lists of DEGs showed an over-representation of cellular processes mainly related to cytoplasmic translation, metabolic processes, biosynthetic processes and gene expression in PCV2b single-infected and in co-infected cells (Fig. 5B).

Moreover, in PCV2b infected cells, a protein-protein interaction enrichment analysis revealed that several DEGs formed a cluster of ribosomal proteins involved in SRP-dependent cotranslational protein targeting to membrane, nonsense mediated decay (NMD) enhanced by the exon junction complex (EJC), membrane trafficking, vesicle-mediated transport, protein stabilization and negative regulation of translation and biosynthetic process (Supplemental Fig. S2). However, the low number of DEGs identified in PRRSV single-infected cells did not allow to detect significantly enriched biological processes or relevant proteins clusters associated to cellular pathways in PRRSV-infected cells. Nonetheless, these results highlight the differential modulation of cellular genes in single-infected and co-infected cells, which could have a potential role in viral replication.

3.6. PCV2b and PRRSV co-infection upregulates DUSP1 mRNA and protein expression

In the present study, PCV2b replication was enhanced after PRRSV co-infection in NPTr-CD163 cells. After the identification of DEGs in the infected cells, functional studies were performed to evaluate the role of a selected DEG in the pathogenesis of PCV2b/PRRSV co-infection. To identify the best candidates for gene functional studies, the list of DEGs was filtered by setting an FDR < 0.001. Among the 19 DEGs having an FDR < 0.001, *DUSP1* was identified among the most up-regulated genes in co-infected cells (Supplemental Table S2). Therefore, *DUSP1* was selected for further studies based also on previous reports showing the involvement of this gene in the replication of several viruses (Cáceres et al., 2013; Choi et al., 2015; Robitaille et al., 2017; Goel et al., 2021; Wilczek et al., 2021). *DUSP1* mRNA and protein expression was determined by RT-qPCR at different time post-infection and by Western blot at 72 hpi, respectively.

As shown in Fig. 6, *DUSP1* mRNA expression was significantly upregulated at all time points post-infection (from 24 to 96 hpi) in co-infected and PRRSV-infected cells compared to mock-infected cells. Moreover, the *DUSP1* mRNA expression was also significantly higher in PCV2b/PRRSV co-infected cells compared to PRRSV infected cells at 48 and 72 hpi. In PCV2b infected cells, *DUSP1* mRNA expression was significantly upregulated at 96 hpi, compared to mock-infected cells. Overall, *DUSP1* mRNA expression in PCV2b infected cells was significantly much weaker compared to PRRSV and PCV2b/PRRSV-infected cells. DUSP1 protein expression was also significantly increased in co-infected cells compared to single-infected cells at 72 hpi, (Fig. 6B and 6C). This study provided evidence that an infection with PCV2b and PRRSV induce upregulation of the expression of *DUSP1* in respiratory epithelial cells (NPTr-CD163 cells), prompting us to decipher how it influenced viral replication during co-infection.

3.7. Transient knockdown of DUSP1 reduces PCV2b replication while it enhances PRRSV replication in PCV2b/PRRSV-infected cells

To determine the effect of *DUSP1* on PCV2b replication in PCV2b/PRRSV-infected cells, DsiRNAs targeting swine *DUSP1* were used to decrease its mRNA expression. *DUSP1* specific DsiRNAs efficiently reduced the gene and protein expression in PCV2b/PRRSV-infected cells (Fig. 7) without having an impact on cell viability (Supplemental Fig. S3).

PCV2b genome copies were significantly reduced in co-infected cells transfected with *DUSP1* DsiRNAs when compared to co-infected cells transfected with scrambled DsiRNA or not transfected (Fig. 8), confirming that *DUSP1* knockdown decreased PCV2b replication in co-infected cells.

On the other hand, the knock-down of *DUSP1* led to a significant increase in PRRSV replication in co-infected cells compared to co-infected cells transfected with scrambled DsiRNA or not transfected (Fig. 8B). While it remains to be understood, this increase in PRRSV genome copies in dually infected cells may have resulted from the

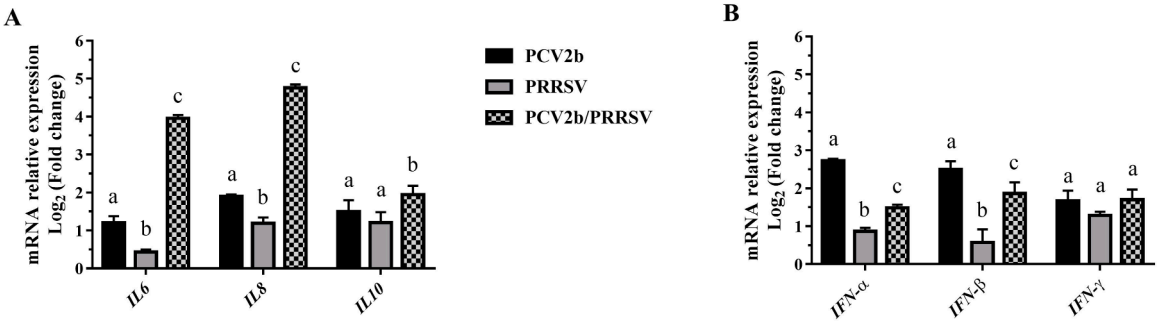

Fig. 4. PCV2b and PRRSV co-infection modulates cytokines mRNA expression in NPTr-CD163 cells. The mRNA expression of *IL6, IL8* and *IL10* (A) and *IFN-α, IFN-β* and *IFN-γ* (B) was determined by qRT-PCR assays. The $2^{-\Delta\Delta Ct}$ method was used to calculate the fold change of cytokines mRNA expression in infected cells with respect to mock-infected cells at 72 hpi. An ordinary two-way ANOVA followed by Tukey's multiple comparisons test was performed to determine the statistical differences between single-infected and co-infected cells. All data are presented with standard deviation (SD) of three biological replicates. Bars labelled with different superscripts letters within the same assay indicates that these sets of data are statistically different ($p < 0.05$).

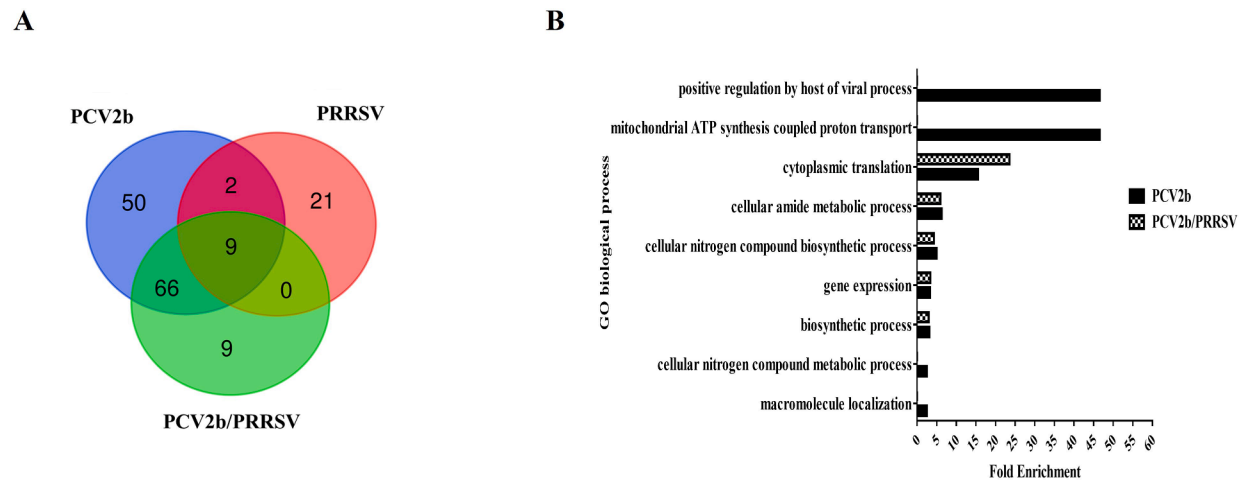

Fig. 5. PCV2b and PRRSV modulate gene expression and biological process in single-infected and co-infected cells. The Venn diagram (A) shows the amount of differentially expressed genes (DEGs) in single-infected and co-infected cells Mock-infected NPTr-CD163 cells were used as a control to identify the DEGs in infected cells. The numbers in overlapping areas represent the amount of DEGs shared by both experimental groups. A False Discovery Rate (FDR) < 0.05 and a 1.5-fold-change cutoff were used to identify the DEGs. GO enrichment analysis was performed with the DEGs identified in PCV2b infected and PCV2b/PRRSV co-infected cells (B). Enriched GO terms (biological process) with FDR value < 0.05 and fold enrichment > 2 are illustrated.

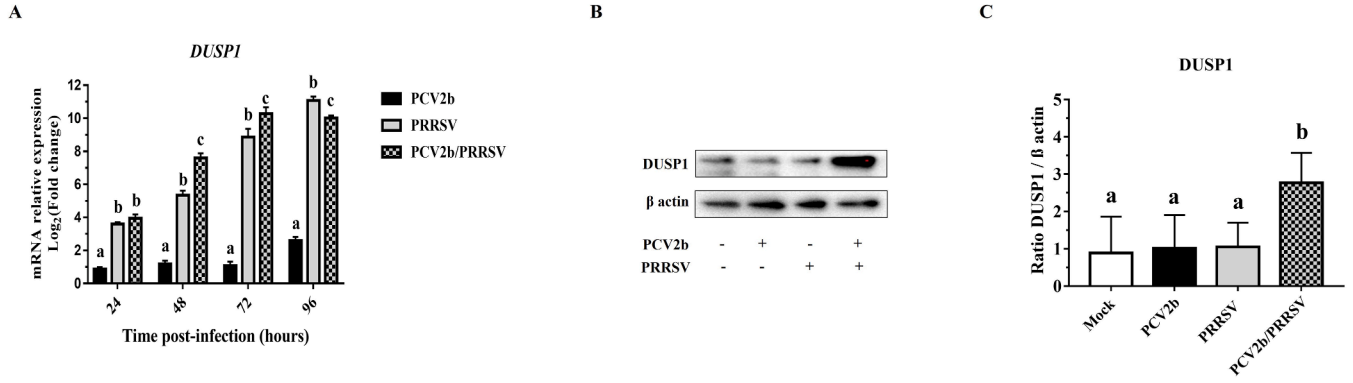

Fig. 6. *DUSP1* expression was differentially modulated in PCV2b and PRRSV single-infected and co-infected NPTr-CD163 cells. *DUSP1* mRNA expression (A) was measure by RT-qPCR at different times post-infection. The $2^{-\Delta\Delta Ct}$ method was used to calculate the fold change of mRNA expression in infected cells with respect to mock-infected cells. DUSP1 protein was quantified by Western blot at 72 hpi (B and C). Statistical analyses were done using one-way ANOVA followed by Tukey's multiple comparisons test. All data are presented with standard deviation (SD) of at least 3 biological replicates. Bars labelled with different superscripts letters within the same assay indicates that these sets of data are statistically different ($p < 0.05$).

reduction in PCV2b genome replication. These results suggest that PCV2b/PRRSV co-infection modulates *DUSP1* expression in infected cells, which in turn, promotes PCV2b replication and negatively impacts the replication of PRRSV in dually infected cells.

3.8. Protein network analysis revealed interaction of DUSP1 with the protein translocation machinery of the endoplasmic reticulum

To analyze the protein-protein interactions involving DUSP1 in single-infected and co-infected cells, physical protein-protein interactions (PPIs) between the corresponding proteins of the identified DEGs in each infection were explored using Metascape (http://metascape.org) (Zhou et al., 2019). The protein-protein interaction enrichment analysis identified that DUSP1 physically interacts with ribosomal proteins RPL24 and RPL38 as wells as with SSR4 (TRAPδ) (Fig. 9).

These proteins belong to a cluster involved in SRP-dependent cotranslational protein targeting to membrane (R-HSA-1,799,339) (Fig. 9 and Supplemental Fig. S2). This cellular pathway couples the synthesis of nascent proteins to its delivery into the endoplasmic reticulum (ER), therefore minimizing the aggregation or misfolding of nascent proteins before they arrive at their cellular destination (Costa et al., 2018). Some studies suggest that the co-translational protein translocation pathway is coupled with the Unfolded Protein Response (UPR) to maintain protein homeostasis in the ER during stress conditions (Plumb et al., 2015; Acosta-Alvear et al., 2018). While it remains to be understood, these observations suggest that DUSP1 interactions with components of the ER protein targeting machinery (RPL38 and SSR4 (TRAPδ)) might have a role in ER stress and the UPR. Further studies are required to elucidate the relevance of this interaction on PCV2b infection in co-infected cells, considering that PCV2b replication can be significantly modulated by ER stress and UPR (Niu et al., 2022).

4. Discussion

PCV2 and/or PRRSV antigens have been found in respiratory epithelial cells of swine co-infected with both viruses (Pol et al., 1991; Halbur et al., 1994; Rossow et al., 1996; Sirinarumitr et al., 2001). Nevertheless, studies concerning the *in vitro* effects of this dual infection in this cell type are scarce, probably due to the lack of a swine respiratory epithelial cell model that allows the simultaneous replication of both viruses. In the present study, *in vitro* effects of PCV2b/PRRSV co-infection were analyzed in the NPTr-CD163 cell line, a swine

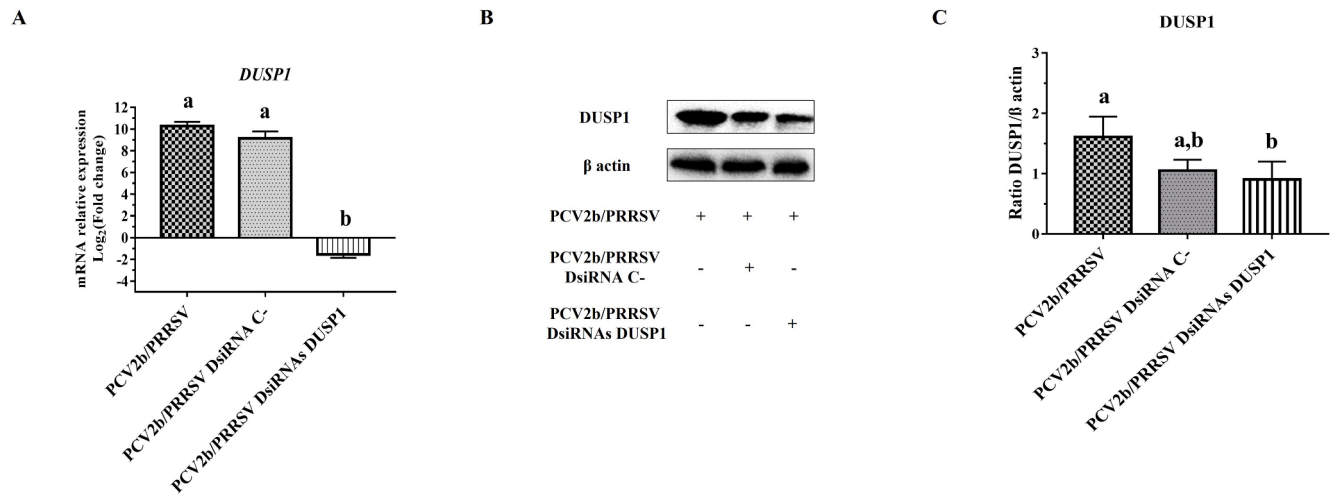

Fig. 7. DsiRNAs targeting swine *DUSP1* decrease gene and protein expression in PCV2b/PRRSV co-infected NPTr-CD163 cells. *DUSP1* mRNA expression (A) was measured by RT-qPCR. The $2^{-\Delta\Delta Ct}$ method was used to calculate the fold change of mRNA expression in infected and/or transfected cells with respect to mock-infected cells. Knockdown of DUSP1 protein was confirmed by Western blot at 72 hpi (B and C). Statistical differences between two groups of samples were determined by paired *t*-test. All data are presented with standard deviation (SD) of at least 3 biological replicates. Bars labelled with different superscripts letters within the same assay indicates that these sets of data are statistically different ($p < 0.05$).

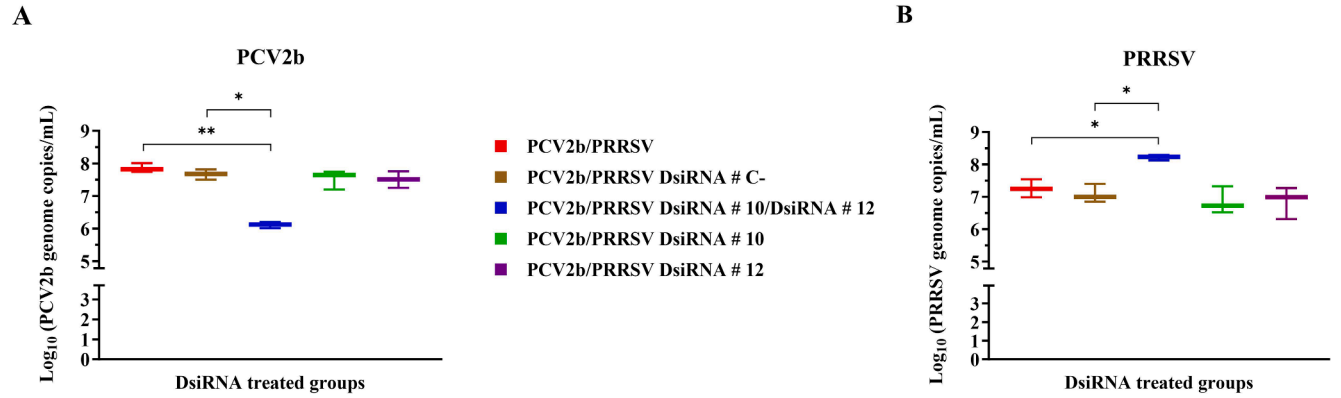

Fig. 8. A transient knockdown of *DUSP1* influences viral replication in PCV2b/PRRSV-infected NPTr-CD163 cells. The PCV2b (A) and the PRRSV (B) genome copy number was measured by qPCR and RT-qPCR, respectively, in co-infected cells after transfection with DsiRNA targeted *DUSP1* or scrambled DsiRNAs. For statistical analysis a one-way ANOVA followed by Tukey's multiple comparisons test was performed. Data are presented with standard deviation (SD) of 3 biological replicates. ** $p < 0.01$, * $p < 0.05$.

respiratory epithelial cell line expressing CD163, the main receptor of PRRSV. This cell line is susceptible to infection by both, PCV2b and PRRSV. It was shown that PCV2b and PRRSV dual infection enhanced PCV2b replication in NPTr-CD163 cells whereas that one of PRRSV was decreased in co-infected cells regarding single-infected cells (Fig. 2). Those results confirm previous studies showing that PCV2b/PRRSV co-infection influences viral replication (Rovira et al., 2002; Sinha et al., 2011; Tsai et al., 2012). Specifically, Sinha et al. (2011) and Rovira et al. (2002) reported an increase in PCV2b viremia and replication in PCV2b/PRRSV co-infected pigs compared to pigs infected only with PCV2b (Rovira et al., 2002; Sinha et al., 2011). However, some studies suggested that PRRSV replication may be favored or not impacted at all in co-infected pigs (Allan et al., 2000b; Rovira et al., 2002; Opriessnig et al., 2008). It is noteworthy to mention that Tsai et al. (2012) demonstrated that PCV2b antigen expression was stable through time in PCV2b single-infected or co-infected porcine alveolar macrophages (PAM) whereas PRRSV antigens expression was decreased in co-infected cells (Tsai et al., 2012). Overall, the different effects of PCV2 and PRRSV dual infection on viral replication reflect the complexity of interactions between PCV2 and PRRSV at the cellular level.

Cell viability was also evaluated after viral infection in the current study. Interestingly, NPTr-CD163 cells possess a very good resilience against PRRSV while none to very low cytopathic effect was observed when they were infected with PRRSV whereas other cells lines such as MARC-145, and PAM cells have been demonstrated to be very sensitive to PRRSV infection (Lévesque et al., 2014; Hernandez Reyes et al., 2018). Our results are in agreement with the results of previous studies (Provost et al., 2012). In fact, Provost et al. (2012) reported that PRRSV infection caused a much higher cytopathic effect (CPE) in PRRSV infected MARC-145 cells compared to SJPL (St-Jude Porcine Lung) infected cells, which expressed no to mild CPE, even when the amount of produced infectious viral particlesd was similar in both infected cell lines. This observation was explained by the phenotypic differences existing between SJPL and MARC-145 cells, leading to differences in cellular response to PRRSV infection. Specifically, Provost et al. (2012) observed an increase in TNF-α mRNA expression in MARC-145 infected cells but not in SJPL infected cells, an observation that, according to the authors, could support the difference observed in CPE.

However, cell viability was decreased in co-infected cells compared to PRRSV single-infected cells. This was not a result of a synergistic effect of both viruses, since no difference was found on the percentage of cell viability between co-infected and PCV2b single-infected cells. This

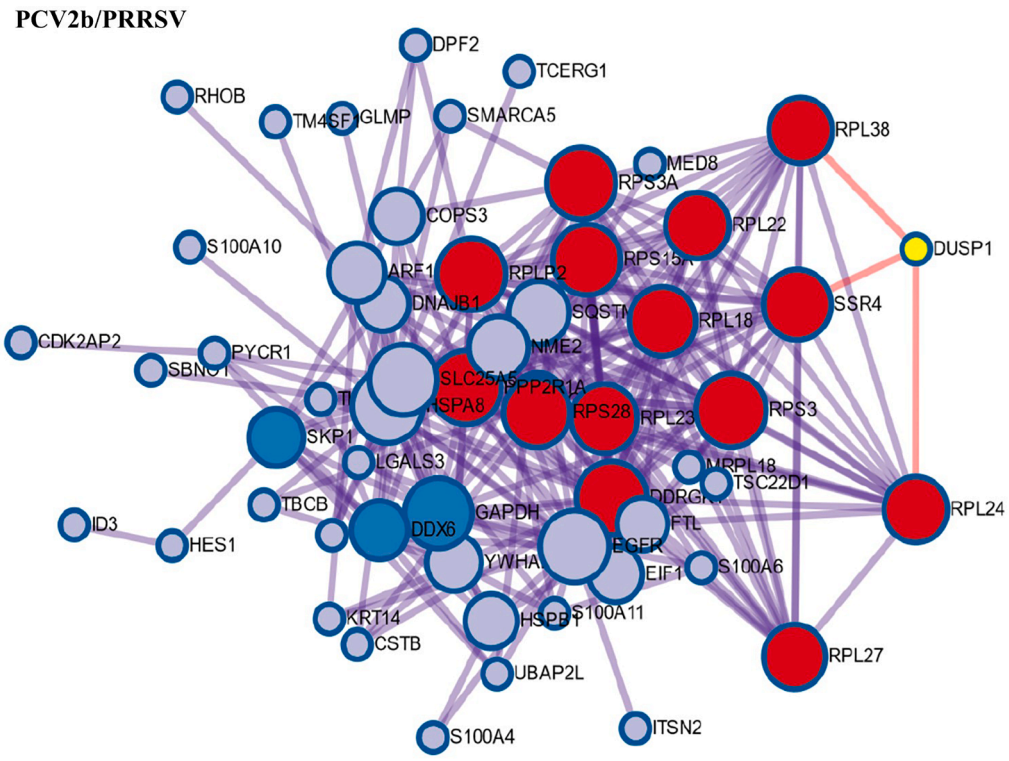

Color	MCODE	GO	Description	Log10(P)
	MCODE_1	R-HSA-1799339	SRP-dependent cotranslational protein targeting to membrane	-27.4
	MCODE_1	R-HSA-975957	Nonsense Mediated Decay (NMD) enhanced by the Exon Junction Complex (EJC)	-27.3
	MCODE_1	R-HSA-927802	Nonsense-Mediated Decay (NMD)	-27.3

Fig. 9. Protein network analysis with the DEGs identified in PCV2b/PRRSV co-infected cells. Predicted physical protein-protein interactions (PPI) between the corresponding proteins of the identified DEGs in PCV2b/PRRSV co-infected cells is shown. DUSP1 protein is highlighted in yellow. Molecular Complex Detection (MCODE) algorithm was applied to identify densely connected network components. MCODE network is assigned a unique color. Pathway and process enrichment analysis has been applied to the MCODE component. The table shows the best-scoring terms by *p*-value retained as the functional description of the corresponding MCODE component.

observation reflects instead the impact of PCV2b infection on the metabolism and functions of NPTr-CD163 cells. It is known that PCV2 impairs the cell survival of NPTr cells (Savard et al., 2015) as well as of other epithelial cell types like PK15 cells (Walia et al., 2014). Therefore, these results confirm previous finding concerning the impact of PCV2b infection on cell viability.

Cytokines mRNA expressions were modulated by PCV2b and PRRSV infections in our cell model. Previous studies have reported an up-regulation of *IL6, IL8*, and *IL10* after PCV2b infection in PK-15 cells, endothelial cells and PAM, respectively (Du et al., 2016; Liu et al., 2019; Gu et al., 2021). Moreover, up-regulation of *IL6, IL8, IL10* and *IFN-γ* has been previously reported after PRRSV infection *in vivo* and in PAM (Meier et al., 2003; Suradhat et al., 2003; Wesley et al., 2006; Song et al., 2013; Liu et al., 2017; Xu et al., 2021). In the present study, no modulation was observed for *IL6* after PRRSV infection. Díaz *et al.* (2012) also observed no modulation of IL6 using ELISA test in pigs experimentally infected with PRRSV (Diaz et al., 2012). Overall, our results in single-infected NPTr-CD163 cells recapitulates the findings of previous reports. Differential modulation of cytokines responses in PCV2 and PRRSV dually infected macrophages, compared to macrophages infected with PCV2 or PRRSV alone, has been previously reported (Tsai et al., 2012). Similar results were obtained in the present study with the NPTr-CD163 cells. The notable increase of *IL6* and *IL8* mRNA expressions observed in co-infected cells suggests that PCV2b and PRRSV dual infection could favor a pro-inflammatory response, which could have an impact in the severity of the respiratory disease in co-infected animals (Van Reeth et al., 2002; Pomorska-Mól et al., 2014; Wilkinson et al., 2015; Turlewicz-Podbielska et al., 2021). It is noteworthy to mention that the results of the present study only refer to a modulation of cytokines expression at mRNA level. Further investigation into the production and release by the cells of these cytokines is required. A reduction of type I Interferon transcriptional expression was observed in co-infected cells compared to PCV2b single-infected cells, probably due to PRRSV infection, which is known to impact type I Interferon responses (Patel et al., 2010). Type I IFN expression is an inherent cell antiviral response that drives the transcription of several genes involved in the initiation of innate and adaptive immune responses leading to viral clearance (Murira and Lamarre, 2016; Teijaro, 2016). While IFN expression can negatively impact the viral replication, for example during PRRSV infection (Brockmeier et al., 2017; Zhu et al., 2021), some studies reported that PCV2 replication can be enhanced in PK-15 cells and 3D4/31 cells after induction of type I and type II IFN responses. Moreover, this IFN-dependent-enhancement of PCV2 replication was blocked by IFN- α or IFN - γ neutralizing antibodies (Meerts et al., 2005). Contrary to these observations, in the current study PCV2b replication increased in the co-infected NPTr-CD163 cells even when the type I IFN transcriptional expression decreased compared to single-infected PCV2b cells (Fig. 4B). These results suggest that other cellular mechanisms could be involved in the modulation of PCV2b infection in co-infected NPTr-CD163 cells.

The 3′ RNA-seq analysis allowed the identification of cellular DEGs with a potential role on viral replication in co-infected cells, such us *DUSP1*. It is known that *DUSP1* is involved in the replication of several viruses, like Vaccinia virus (VACV), JC polyomavirus (JCPyV), Hepatitis C virus (HCV), Human respiratory syncytial virus (RSV), Sendai virus

(SeV) and SARS-CoV-2 virus (Cáceres et al., 2013; Choi et al., 2015; Robitaille et al., 2017; Goel et al., 2021; Wilczek et al., 2021). In the present study, *DUSP1* mRNA and protein expression was upregulated in co-infected NPTr-CD163 cells compared to PCV2b single infected cells. Moreover, transient knockdown of *DUSP1* expression significantly reduced PCV2b replication in dually infected cells, suggesting a role for *DUSP1* in the modulation of PCV2b in co-infected cells.

It has been reported that PCV2 can activate anti-apoptotic mechanisms at the early stage of infection to favors viral replication while inducing pro-apoptotic mechanisms in the late stage for release and dissemination of virions (Pan et al., 2018). It is known that PCV2 triggers ER stress and the UPR in PK-15 cells and PAM (Ouyang et al., 2019; Zhang et al., 2019; Wang et al., 2021), wich leads to apoptosis and in turn facilitates viral replication (Niu et al., 2022). PCV2 induction of ER stress and UPR also involves elevation of cytosolic calcium, which causes alteration of Ca^{2+} homeostasis leading to apoptosis (Zhang et al., 2019; Wang et al., 2021). Interestingly, some studies reported that *DUSP1* expression modulates apoptosis rate in different types of cells (Fu et al., 2019; Yang et al., 2019). Moreover, Robitaille et al. (2017) showed that *DUSP1* has a pro-apoptotic function independently of JNK and p38 pathways during SeV infection [45]. Considering these observations, it could be interesting to determine whether *DUSP1* modulates PCV2b replication in NPTr-CD163 co-infected cells via modulation of apoptosis and ER stress.

On the other hand, the *in silico* analysis of protein-protein interaction networks on co-infected cells revealed that DUSP1 interacts with ribosomal protein RLP38 and SSR4 TRAP subunit, which are both involved in the translocon complex. TRAP/ribosome complex promotes the open gate of the Sec61 protein-conducting channel for favorable polypeptide insertion through this channel and allows Ca^{2+} leakage (Hamman et al., 1997; Van Coppenolle et al., 2004; Karki et al., 2022). Moreover, it is known that Sec61 translocon complex has a role in ER stress and UPR induction, (Sicari et al., 2020; Adams et al., 2019; Read and Schröder, 2021). The results of the protein-protein interaction networks analysis in the present study raise the question of whether DUSP1 binding to RPL38 and SSR4 (TRAPδ) might have an impact on the dynamics of protein translocation or Ca^{2+} leakage from the ER and ultimately the ER homeostasis. Overall, further studies are needed to confirm if *DUSP1* up-regulation in PCV2b/PRRSV co-infected cells mediates PCV2b enhanced replication via ER stress, UPR and apoptotic pathways.

5. Conclusions

In the current study, NPTr-CD163 cells were used as an *in vitro* model to study PCV2b/PRRSV co- infection. Our results confirmed that in cells previously infected with PCV2b, a subsequent infection with PRRSV can enhance PCV2b replication, whereas PRRSV replication is negatively impacted. Differential modulation of cytokines transcriptional expression and cellular genes having a role in virus replication could explain this effect in co-infected NPTr-CD163 cells. Specifically, this study highlights a possible role of DUSP1 in the modulation of PCV2b replication during PCV2b/PRRSV *in vitro* co-infection. However, further studies are needed to confirm the role of DUSP1 on viral pathogenesis within PCV2b and PRRSV infected pigs. Overall, our results provide new insights on PCV2b and PRRSV interactions.

Funding

This project was funded by a Natural Sciences and Engineering Research Council of Canada (NSERC) discovery grant (number RGPIN-2017-05240). C.A. Gagnon was financially supported by a Canadian Swine Research and Development Cluster (CSRDC) research project, Les éleveurs de porcs du Québec and by Probiotech International (number 1781). Y. Burgher and M.J. Pesant were recipients of a graduate student scholarship from the Fonds de recherche du Québec – Nature et technologie (FRQNT). Both were also recipients of graduate student scholarships from the Swine and poultry infectious diseases research center (Centre de recherche en infectiologie porcine et avicole, CRIPA-FRQNT) and of different graduate student merit scholarships for Graduate and Postdoctoral Studies from the Université de Montréal.

CRediT authorship contribution statement

Yaima Burgher-Pulgaron: Formal analysis, Methodology, Data curation, Writing – original draft, Writing – review & editing. **Chantale Provost:** Data curation, Supervision, Formal analysis, Methodology, Writing – review & editing. **Fernando Alvarez:** Data curation, Formal analysis, Writing – review & editing. **Europa Meza-Serrano:** Methodology. **Marie-Jeanne Pesant:** Methodology, Formal analysis, Writing – review & editing. **Christopher A. Price:** Supervision, Methodology. **Carl A. Gagnon:** Conceptualization, Funding acquisition, Project administration, Resources, Supervision, Writing – review & editing.

Declaration of Competing Interest

The authors declare that they have no known competing financial interests or personal relationships that could have appeared to influence the work reported in this paper.

Acknowledgments

The authors would like to acknowledge the support of current and former post-graduate students of Dr Gagnon's Laboratories, Faculté de médecine vétérinaire, Université de Montréal.

Supplementary materials

Supplementary material associated with this article can be found, in the online version, at doi:10.1016/j.virusres.2023.199282.

References

Acosta-Alvear, D., Karagöz, G.E., Fröhlich, F., Li, H., Walther, T.C., Walter, P., 2018. The unfolded protein response and endoplasmic reticulum protein targeting machineries converge on the stress sensor IRE1. eLife 7, e43036.

Adams, C.J., Kopp, M.C., Larburu, N., Nowak, P.R., Ali, M.M., 2019. Structure and molecular mechanism of ER stress signaling by the unfolded protein response signal activator IRE1. Front Mol. Biosci. 6, 11.

Allan, G.M., Ellis, J.A., 2000. Porcine circoviruses: a review. J. Vet. Diagn. Invest. 12 (1), 3–14.

Allan, G.M., McNeilly, E., Kennedy, S., Meehan, B., Moffett, D., Malone, F., Ellis, J., Krakowka, S., 2000a. PCV-2-associated PDNS in Northern Ireland in 1990. Porcine dermatitis and nephropathy syndrome. Vet. Rec. 146 (24), 711–712.

Allan, G.M., McNeilly, F., Ellis, J., Krakowka, S., Meehan, B., McNair, I., Walker, I., Kennedy, S., 2000b. Experimental infection of colostrum deprived piglets with porcine circovirus 2 (PCV2) and porcine reproductive and respiratory syndrome virus (PRRSV) potentiates PCV2 replication. Arch. Virol. 145 (11), 2421–2429.

Ashburner, M., Ball, C.A., Blake, J.A., Botstein, D., Butler, H., Cherry, J.M., Davis, A.P., Dolinski, K., Dwight, S.S., Eppig, J.T., 2000. Gene ontology: tool for the unification of biology. Nat. Genet. 25 (1), 25–29.

Brockmeier, S.L., Halbur, P.G., Thacker, E.L., 2002. Porcine Respiratory Disease Complex. Wiley Online Library, Hoboken, NJ, USA, pp. 231–258.

Brockmeier, S.L., Loving, C.L., Eberle, K.C., Hau, S.J., Buckley, A., Van Geelen, A., Montiel, N.A., Nicholson, T., Lager, K.M., 2017. Interferon alpha inhibits replication of a live-attenuated porcine reproductive and respiratory syndrome virus vaccine preventing development of an adaptive immune response in swine. Vet. Microbiol. 212, 48–51.

Burgher Pulgaron, Y., Provost, C., Pesant, M.J., Gagnon, C.A., 2023. Porcine circovirus modulates swine influenza virus replication in pig tracheal epithelial cells and porcine alveolar macrophages. Viruses 15 (5), 1207.

Cáceres, A., Perdiguero, B., Gómez, C.E., Cepeda, M.V., Caelles, C., Sorzano, C.O., Esteban, M., 2013. Involvement of the cellular phosphatase DUSP1 in vaccinia virus infection. PLoS Pathog. 9 (11), e1003719.

Chang, H.W., Jeng, C.R., Liu, J.J., Lin, T.L., Chang, C.C., Chia, M.Y., Tsai, Y.C., Pang, V. F., 2005. Reduction of porcine reproductive and respiratory syndrome virus (PRRSV) infection in swine alveolar macrophages by porcine circovirus 2 (PCV2)-induced interferon-alpha. Vet. Microbiol. 108 (3–4), 167–177.

Choi, J.E., Kwon, J.H., Kim, J.H., Hur, W., Sung, P.S., Choi, S.W., Yoon, S.K., 2015. Suppression of dual specificity phosphatase I expression inhibits hepatitis C virus replication. PLoS One 10 (3), e0119172.

Costa, E.A., Subramanian, K., Nunnari, J., Weissman, J.S., 2018. Defining the physiological role of SRP in protein-targeting efficiency and specificity. Science 359 (6376), 689–692.
Dan, A., Molnar, T., Biksi, I., Glavits, R., Shaheim, M., Harrach, B., 2003. Characterisation of Hungarian porcine circovirus 2 genomes associated with PMWS and PDNS cases. Acta Vet. Hung. 51 (4), 551–562.
Dea, S., Gagnon, C.A., Mardassi, H., Milane, G., 1996. Antigenic variability among North American and European strains of porcine reproductive and respiratory syndrome virus as defined by monoclonal antibodies to the matrix protein. J. Clin. Microbiol. 34 (6), 1488–1493.
Diaz, I., Gimeno, M., Darwich, L., Navarro, N., Kuzemtseva, L., Lopez, S., Galindo, I., Segales, J., Martin, M., Pujols, J., Mateu, E., 2012. Characterization of homologous and heterologous adaptive immune responses in porcine reproductive and respiratory syndrome virus infection. Vet. Res. 43, 30.
Dorr, P.M., Baker, R.B., Almond, G.W., Wayne, S.R., Gebreyes, W.A., 2007. Epidemiologic assessment of porcine circovirus type 2 coinfection with other pathogens in swine. J. Am. Vet. Med. Assoc. 230 (2), 244–250.
Du, Q., Huang, Y., Wang, T., Zhang, X., Chen, Y., Cui, B., Li, D., Zhao, X., Zhang, W., Chang, L., Tong, D, 2016. Porcine circovirus type 2 activates PI3K/Akt and p38 MAPK pathways to promote interleukin-10 production in macrophages via Cap interaction of gC1qR. Oncotarget 7 (14), 17492–17507.
Fan, P., Wei, Y., Guo, L., Wu, H., Huang, L., Liu, J., Liu, C., 2013. Synergistic effects of sequential infection with highly pathogenic porcine reproductive and respiratory syndrome virus and porcine circovirus type 2. Virol. J. 10, 265.
Fraile, L., Calsamiglia, M., Mateu, E., Espinal, A., Cuxart, A., Seminati, C., Martin, M., Domingo, M., Segales, J., 2009. Prevalence of infection with porcine circovirus-2 (PCV-2) and porcine reproductive and respiratory syndrome virus (PRRSV) in an integrated swine production system experiencing postweaning multisystemic wasting syndrome. Can. J. Vet. Res. 73 (4), 308–312.
Franzo, G., Segales, J., 2018. Porcine circovirus 2 (PCV-2) genotype update and proposal of a new genotyping methodology. PLoS One 13 (12), e0208585.
Fu, X.h., Chen, C.z., Li, S., Han, D.x., Wang, Y.j., Yuan, B., Gao, Y., Zhang, J.b., Jiang, H., 2019. Dual-specificity phosphatase 1 regulates cell cycle progression and apoptosis in cumulus cells by affecting mitochondrial function, oxidative stress, and autophagy. Am. J. Physiol.-Cell Physiol. 317 (6), C1183–C1193.
Gagnon, C.A., Lachapelle, G., Langelier, Y., Massie, B., Dea, S., 2003. Adenoviral-expressed GP5 of porcine respiratory and reproductive syndrome virus differs in its cellular maturation from the authentic viral protein but maintains known biological functions. Arch. Virol. 148 (5), 951–972.
Gagnon, C.A., Tremblay, D., Tijssen, P., Venne, M.H., Houde, A., Elahi, S.M., 2007. The emergence of porcine circovirus 2b genotype (PCV-2b) in swine in Canada. Can. Vet. J. 48 (8), 811–819.
Gillespie, J., Opriessnig, T., Meng, X., Pelzer, K., Buechner-Maxwell, V., 2009. Porcine circovirus type 2 and porcine circovirus-associated disease. J. Vet. Intern. Med. 23 (6), 1151–1163.
Goel, S., Saheb Sharif-Askari, F., Saheb Sharif Askari, N., Madkhana, B., Alwaa, A.M., Mahboub, B., Zakeri, A.M., Ratemi, E., Hamoudi, R., Hamid, Q., 2021. SARS-CoV-2 switches 'on'MAPK and NFκB signaling via the reduction of nuclear DUSP1 and DUSP5 expression. Front. Pharmacol. 12, 631879.
Gu, C., Gao, X., Guo, D., Wang, J., Wu, Q., Nepovimova, E., Wu, W., Kuca, K., 2021. Combined effect of deoxynivalenol (DON) and porcine circovirus type 2 (Pcv2) on inflammatory cytokine mRNA expression. Toxins (Basel) 13 (6).
Günther, J., Seyfert, H.M., 2018. The first line of defence: insights into mechanisms and relevance of phagocytosis in epithelial cells. Semin. Immunopathol. 40 (6), 555–565.
Halbur, P.G., Andrews, J.J., Huffman, E.L., Paul, P.S., Meng, X.J., Niyo, Y., 1994. Development of a streptavidin-biotin immunoperoxidase procedure for the detection of porcine reproductive and respiratory syndrome virus antigen in porcine lung. J. Vet. Diagn. Invest. 6 (2), 254–257.
Hamman, B.D., Chen, J.C., Johnson, E.E., Johnson, A.E., 1997. The aqueous pore through the translocon has a diameter of 40–60Å during cotranslational protein translocation at the ER membrane. Cell 89 (4), 535–544.
Hernandez Reyes, Y., Provost, C., Traesel, C.K., Jacques, M., Gagnon, C.A., 2018. Actinobacillus pleuropneumoniae culture supernatant antiviral effect against porcine reproductive and respiratory syndrome virus occurs prior to the viral genome replication and transcription through actin depolymerization. J. Med. Microbiol. 67 (2), 249–264.
Hu, Y., Zhan, Y., Wang, D., Xie, X., Liu, T., Liu, W., Wang, N., Deng, Z., Lei, H., Yang, Y., Wang, A, 2017. Evidence of natural co-infection with PCV2b subtypes *in vivo*. Arch. Virol. 162 (7), 2015–2020.
Huang, D., Sherman, B., Lempicki, R., 2009. Systematic and integrative analysis of large gene lists using DAVID Bioinformatics Resources. Nat. Protoc. 4 (1), 44–57.
Kärber, G., 1931. Tabellen zur näherungsweisen Bestimmung von Titern." Naunyn Schmiedebergs Arch. Exp. Pathol. Pharmakol. 162, 480.
Karki, S., Javanainen, M., Tranter, D., Rehan, S., Huiskonen, J.T., Happonen, L., Paavilainen, V., 2022. Molecular view of ER membrane remodeling by the Sec61/TRAP translocon. Biorxiv. https://doi.org/10.1101/2022.09.30.510141.
Kekarainen, T., McCullough, K., Fort, M., Fossum, C., Segales, J., Allan, G.M., 2010. Immune responses and vaccine-induced immunity against Porcine circovirus type 2. Vet. Immunol. Immunopathol. 136 (3–4), 185–193.
Kim, J., Chung, H.K., Chae, C., 2003. Association of porcine circovirus 2 with porcine respiratory disease complex. Vet. J. 166 (3), 251–256.
Lefkowitz, E., Dempsey, D., Hendrickson, R.C., Orton, R.J., Siddell, S.G., Smith, D.B., 2017. Virus taxonomy: the database of the International Committee on Taxonomy of Viruses (ICTV). Nucl. Acids. Res. 46 (D1), D708–D717.
Lefkowitz, E.J., Dempsey, D.M., Hendrickson, R.C., Orton, R.J., Siddell, S.G., Smith, D.B., 2018. Virus taxonomy: the database of the International Committee on Taxonomy of Viruses (ICTV). Nucl. Acids. Res. 46 (D1), D708–D717.
Lévesque, C., Provost, C., Labrie, J., Hernandez Reyes, Y., Burciaga Nava, J.A., Gagnon, C.A., Jacques, M., 2014. Actinobacillus pleuropneumoniae possesses an antiviral activity against porcine reproductive and respiratory syndrome virus. PLoS One 9 (5), e98434.
Link, E.K., Eddicks, M., Nan, L., Ritzmann, M., Sutter, G., Fux, R., 2021. Discriminating the eight genotypes of the porcine circovirus type 2 with TaqMan-based real-time PCR. Virol. J. 18 (1), 70.
Liu, S., Li, Q., Qiao, J., Wang, J., Cui, D., Gu, K., Zhou, S., Li, H., 2019. Endothelial IL-8 induced by porcine circovirus type 2 affects dendritic cell maturation and antigen-presenting function. Virol. J. 16 (1), 154.
Liu, Y., Du, Y., Wang, H., Du, L., Feng, W.H., 2017. Porcine reproductive and respiratory syndrome virus (PRRSV) up-regulates IL-8 expression through TAK-1/JNK/AP-1 pathways. Virology 506, 64–72.
Meerts, P., Misinzo, G., Nauwynck, H., 2005. Enhancement of porcine circovirus 2 replication in porcine cell lines by IFN-γ before and after treatment and by IFN-α after treatment. J. Interferon 25 (11), 684–693.
Meier, W.A., Galeota, J., Osorio, F.A., Husmann, R.J., Schnitzlein, W.M., Zuckermann, F. A., 2003. Gradual development of the interferon-gamma response of swine to porcine reproductive and respiratory syndrome virus infection or vaccination. Virology 309 (1), 18–31.
Miller, L.C., Fleming, D.S., Lager, K.M., 2020. Comparison of the Transcriptome response within the swine tracheobronchial Lymphnode following infection with PRRSV, PCV-2 or IAV-S. Pathogens 9 (2).
Murira, A., Lamarre, A., 2016. Type-I interferon responses: from friend to foe in the battle against chronic viral infection. Front. Immunol. 7, 609.
Neumann, E.J., Kliebenstein, J.B., Johnson, C.D., Mabry, J.W., Bush, E.J., Seitzinger, A. H., Green, A.L., Zimmerman, J.J., 2005. Assessment of the economic impact of porcine reproductive and respiratory syndrome on swine production in the United States. J. Am. Vet. Med. Assoc. 227 (3), 385–392.
Niu, G., Chen, S., Li, X., Zhang, L., Ren, L., 2022. Advances in crosstalk between porcine circoviruses and host. Viruses 14 (7), 1419.
Opriessnig, T., Gauger, P.C., Faaberg, K.S., Shen, H., Beach, N.M., Meng, X.J., Wang, C., Halbur, P.G., 2012. Effect of porcine circovirus type 2a or 2b on infection kinetics and pathogenicity of two genetically divergent strains of porcine reproductive and respiratory syndrome virus in the conventional pig model. Vet. Microbiol. 158 (1–2), 69–81.
Opriessnig, T., Gimenez-Lirola, L.G., Halbur, P.G., 2011. Polymicrobial respiratory disease in pigs. Anim. Health Res. Rev. 12 (2), 133–148.
Opriessnig, T., Halbur, P.G., 2012. Concurrent infections are important for expression of porcine circovirus associated disease. Virus Res. 164 (1–2), 20–32.
Opriessnig, T., Madson, D.M., Prickett, J.R., Kuhar, D., Lunney, J.K., Elsener, J., Halbur, P.G., 2008. Effect of porcine circovirus type 2 (PCV2) vaccination on porcine reproductive and respiratory syndrome virus (PRRSV) and PCV2 coinfection. Vet. Microbiol. 131 (1–2), 103–114.
Oshlack, A., Robinson, M.D., Young, M.D., 2010. From RNA-seq reads to differential expression results. Genome Biol. 11, 1–10.
Ouyang, Y., Xu, L., Lv, J., Hou, Y., Fan, Z., Xu, P., Jiang, Y., Wu, M., Li, R., Zhang, Y., Guo, K., 2019. Porcine circovirus type 2 ORF5 protein induces endoplasmic reticulum stress and unfolded protein response in porcine alveolar macrophages. Arch. Virol. 164 (5), 1323–1334.
Pallares, F.J., Halbur, P.G., Opriessnig, T., Sorden, S.D., Villar, D., Janke, B.H., Yaeger, M.J., Larson, D.J., Schwartz, K.J., Yoon, K.J., Hoffman, L.J., 2002. Porcine circovirus type 2 (PCV-2) coinfections in US field cases of postweaning multisystemic wasting syndrome (PMWS). J. Vet. Diagn. Invest. 14 (6), 515–519.
Pan, Y., Li, P., Jia, R., Wang, M., Yin, Z., Cheng, A., 2018. Regulation of apoptosis during porcine circovirus type 2 infection. Front. Microbiol. 9, 2086.
Park, C., Seo, H.W., Park, S.J., Han, K., Chae, C., 2014. Comparison of porcine circovirus type 2 (PCV2)-associated lesions produced by co-infection between two genotypes of PCV2 and two genotypes of porcine reproductive and respiratory syndrome virus. J. Gen. Virol. 95 (Pt 11), 2486–2494.
Patel, D., Nan, Y., Shen, M., Ritthipichai, K., Zhu, X., Zhang, Y.J., 2010. Porcine reproductive and respiratory syndrome virus inhibits type I interferon signaling by blocking STAT1/STAT2 nuclear translocation. J. Virol. 84 (21), 11045–11055.
Plumb, R., Zhang, Z.R., Appathurai, S., Mariappan, M., 2015. A functional link between the co-translational protein translocation pathway and the UPR. eLife 4, e07426.
Pol, J., Van Dijk, J., Wensvoort, G., Terpstra, C., 1991. Pathological, ultrastructural, and immunohistochemical changes caused by Lelystad virus in experimentally induced infections of mystery swine disease (synonym: porcine epidemic abortion and respiratory syndrome (PEARS)). Vet. Q. 13 (3), 137–143.
Pomorska-Mól, M., Markowska-Daniel, I., Kwit, K., Czyżewska, E., Dors, A., Rachubik, J., Pejsak, Z., 2014. Immune and inflammatory response in pigs during acute influenza caused by H1N1 swine influenza virus. Arch. Virol. 159, 2605–2614.
Provost, C., Hamonic, G., Gagnon, C.A., Meurens, F., 2017. Dual infections of CD163 expressing NPTr epithelial cells with influenza A virus and PRRSV. Vet. Microbiol. 207, 143–148.
Provost, C., Jia, J.J., Music, N., Lévesque, C., Lebel, M.È., del Castillo, J.R., Jacques, M., Gagnon, C.A., 2012. Identification of a new cell line permissive to porcine reproductive and respiratory syndrome virus infection and replication which is phenotypically distinct from MARC-145 cell line. Virol. J. 9 (1), 1–14.
Read, A., Schröder, M., 2021. The unfolded protein response: an overview. Biology (Basel) 10 (5), 384.
Robinson, M.D., Oshlack, A., 2010. A scaling normalization method for differential expression analysis of RNA-seq data. Genome Biol. 11 (3), 1–9.

Robitaille, A.C., Caron, E., Zucchini, N., Mukawera, E., Adam, D., Mariani, M.K., Gélinas, A., Fortin, A., Brochiero, E., Grandvaux, N., 2017. DUSP1 regulates apoptosis and cell migration, but not the JIP1-protected cytokine response, during Respiratory Syncytial Virus and Sendai Virus infection. Sci. Rep. 7 (1), 1–15.
Rossow, K.D., Benfield, D.A., Goyal, S.M., Nelson, E.A., Christopher-Hennings, J., Collins, J.E., 1996. Chronological immunohistochemical detection and localization of porcine reproductive and respiratory syndrome virus in gnotobiotic pigs. Vet. Pathol. 33 (5), 551–556.
Rovira, A., Balasch, M., Segales, J., Garcia, L., Plana-Duran, J., Rosell, C., Ellerbrok, H., Mankertz, A., Domingo, M., 2002. Experimental inoculation of conventional pigs with porcine reproductive and respiratory syndrome virus and porcine circovirus 2. J. Virol. 76 (7), 3232–3239.
Sang, Y., Rowland, R.R., Blecha, F., 2011. Interaction between innate immunity and porcine reproductive and respiratory syndrome virus. Anim. Health Res. Rev. 12 (2), 149–167.
Savard, C., Provost, C., Alvarez, F., Pinilla, V., Music, N., Jacques, M., Gagnon, C.A., Chorfi, Y., 2015. Effect of deoxynivalenol (DON) mycotoxin on *in vivo* and *in vitro* porcine circovirus type 2 infections. Vet. Microbiol. 176 (3–4), 257–267.
Segales, J., Calsamiglia, M., Rosell, C., Soler, M., Maldonado, J., Martin, M., Domingo, M., 2002. Porcine reproductive and respiratory syndrome virus (PRRSV) infection status in pigs naturally affected with post-weaning multisystemic wasting syndrome (PMWS) in Spain. Vet. Microbiol. 85 (1), 23–30.
Shi, K., Li, H., Guo, X., Ge, X., Jia, H., Zheng, S., Yang, H., 2008. Changes in peripheral blood leukocyte subpopulations in piglets co-infected experimentally with porcine reproductive and respiratory syndrome virus and porcine circovirus type 2. Vet. Microbiol. 129 (3–4), 367–377.
Sicari, D., Delaunay-Moisan, A., Combettes, L., Chevet, E., Igbaria, A., 2020. A guide to assessing endoplasmic reticulum homeostasis and stress in mammalian systems. FEBS J. 287 (1), 27–42.
Sinha, A., Shen, H.G., Schalk, S., Beach, N.M., Huang, Y.W., Meng, X.J., Halbur, P.G., Opriessnig, T., 2011. Porcine reproductive and respiratory syndrome virus (PRRSV) influences infection dynamics of porcine circovirus type 2 (PCV2) subtypes PCV2a and PCV2b by prolonging PCV2 viremia and shedding. Vet. Microbiol. 152 (3–4), 235–246.
Sirinarumitr, T., Sorden, S.D., Morozov, I., Paul, P.S., 2001. Double *in situ* hybridization for simultaneous detection of porcine reproductive and respiratory syndrome virus (PRRSV) and porcine circovirus (PCV). J. Vet. Diagn. Invest. 13 (1), 68–71.
Solano, G.I., Segalés, J., Collins, J.E., Molitor, T.W., Pijoan, C., 1997. Porcine reproductive and respiratory syndrome virus (PRRSv) interaction with Haemophilus parasuis. Vet. Microbiol. 55 (1–4), 247–257.
Song, S., Bi, J., Wang, D., Fang, L., Zhang, L., Li, F., Chen, H., Xiao, S., 2013. Porcine reproductive and respiratory syndrome virus infection activates IL-10 production through NF-kappaB and p38 MAPK pathways in porcine alveolar macrophages. Dev. Comp. Immunol. 39 (3), 265–272.
Sorden, S., Harms, P., Sirinarumitr, T., Morozov, I., Halbur, P., Yoon, K., Paul, P., 1998. Porcine circovirus and PRRSV co-infection in pigs with chronic bronchointerstitial pneumonia and lymphoid depletion: an emerging syndrome in midwestern swine. In: Proceedings of the Annual Meeting of the American Association of Veterinary Laboratory Diagnosticians. American Association of Veterinary Laboratory Diagnosticians, Minneapolis, Minn, p. 75.
Spearman, C., 1909. Review of The method of 'right and wrong cases'('Constant stimuli') without gauss's formula. Psychol. Bull. 6 (1), 27–28.
Supek, F., Bošnjak, M., Škunca, N., Šmuc, T., 2011. REVIGO summarizes and visualizes long lists of gene ontology terms. PLoS One 6 (7).
Suradhat, S., Thanawongnuwech, R., Poovorawan, Y., 2003. Upregulation of IL-10 gene expression in porcine peripheral blood mononuclear cells by porcine reproductive and respiratory syndrome virus. J. Gen. Virol. 84 (Pt 2), 453–459.
Teijaro, J.R., 2016. Type I interferons in viral control and immune regulation. Curr. Opin. Virol. 16, 31–40.
Thanawongnuwech, R., Brown, G., Halbur, P., Roth, J., Royer, R., Thacker, B., 2000a. Pathogenesis of porcine reproductive and respiratory syndrome virus-induced increase in susceptibility to Streptococcus suis infection. Vet. Pathol. 37 (2), 143–152.
Thanawongnuwech, R., Halbur, P.G., Thacker, E.L., 2000b. The role of pulmonary intravascular macrophages in porcine reproductive and respiratory syndrome virus infection. Anim. Health Res. Rev. 1 (2), 95–102.
The-Gene-Ontology-Consortium, 2021. The gene ontology resource: enriching a GOld mine. Nucleic. Acids. Res. 49 (D1), D325–D334.
Thomson, J., Smith, B., Allan, G., McNeilly, F., McVicar, C., 2000. PDNS, PMWS and porcine circovirus type 2 in Scotland. Porcine dermatitis and nephropathy syndrome. Post-weaning multisystemic wasting syndrome. Vet. Rec. 146 (22), 651–652.
Tsai, Y.C., Chang, H.W., Jeng, C.R., Lin, T.L., Lin, C.M., Wan, C.H., Pang, V.F., 2012. The effect of infection order of porcine circovirus type 2 and porcine reproductive and respiratory syndrome virus on dually infected swine alveolar macrophages. BMC Vet. Res. 8, 174.
Turlewicz-Podbielska, H., Czyżewska-Dors, E., Pomorska-Mól, M., 2021. Respiratory viral infections drive different lung cytokine profiles in pigs. BMC Vet. Res. 17 (1), 1–8.
Van Coppenolle, F., Vanden Abeele, F., Slomianny, C., Flourakis, M., Hesketh, J., Dewailly, E., Prevarskaya, N., 2004. Ribosome-translocon complex mediates calcium leakage from endoplasmic reticulum stores. J. Cell. Sci. 117 (18), 4135–4142.
Van Reeth, K., Van Gucht, S., Pensaert, M., 2002. In vivo studies on cytokine involvement during acute viral respiratory disease of swine: troublesome but rewarding. Vet. Immunol. 87 (3–4), 161–168.
Vareille, M., Kieninger, E., Edwards, M.R., Regamey, N., 2011. The airway epithelium: soldier in the fight against respiratory viruses. Clin. Microbiol. Rev. 24 (1), 210–229.
Walia, R., Dardari, R., Chaiyakul, M., Czub, M., 2014. Porcine circovirus-2 capsid protein induces cell death in PK15 cells. Virology 468-470, 126–132.
Wang, S., Li, C., Sun, P., Shi, J., Wu, X., Liu, C., Peng, Z., Han, H., Xu, S., Yang, Y., Tian, Y., Li, J., He, H., Li, J., Wang, Z., 2021. PCV2 triggers PK-15 cell apoptosis through the PLC-IP3R-Ca(2+) signaling pathway. Front. Microbiol. 12, 674907.
Wang, Y., Noll, L., Lu, N., Porter, E., Stoy, C., Zheng, W., Liu, X., Peddireddi, L., Niederwerder, M., Bai, J., 2020. Genetic diversity and prevalence of porcine circovirus type 3 (PCV3) and type 2 (PCV2) in the Midwest of the USA during 2016-2018. Transbound Emerg. Dis. 67 (3), 1284–1294.
Wellenberg, G.J., Stockhofe-Zurwieden, N., Boersma, W.J., De Jong, M.F., Elbers, A.R., 2004. The presence of co-infections in pigs with clinical signs of PMWS in the Netherlands: a case-control study. Res. Vet. Sci. 77 (2), 177–184.
Wesley, R.D., Lager, K.M., Kehrli Jr., M.E., 2006. Infection with Porcine reproductive and respiratory syndrome virus stimulates an early gamma interferon response in the serum of pigs. Can. J. Vet. Res. 70 (3), 176–182.
Wilczek, M.P., Armstrong, F.J., Geohegan, R.P., Mayberry, C.L., DuShane, J.K., King, B. L., Maginnis, M.S., 2021. The MAPK/ERK pathway and the role of DUSP1 in JCPyV infection of primary astrocytes. Viruses 13 (9), 1834.
Wilkinson, J.M., Gunvaldsen, R.E., Detmer, S.E., Dyck, M.K., Dixon, W.T., Foxcroft, G.R., Plastow, G.S., Harding, J.C., 2015. Transcriptomic and epigenetic profiling of the lung of influenza-infected pigs: a comparison of different birth weight and susceptibility groups. PLoS One 10 (9), e0138653.
Xu, Y., Wang, H., Zhang, X., Zheng, X., Zhu, Y., Han, H., Feng, W.H., 2021. Highly pathogenic porcine reproductive and respiratory syndrome virus (HP-PRRSV) induces IL-6 production through TAK-1/JNK/AP-1 and TAK-1/NF-kappaB signaling pathways. Vet. Microbiol. 256, 109061.
Yang, J., Sun, L., Han, J., Zheng, W., Peng, W., 2019. DUSP1/MKP-1 regulates proliferation and apoptosis in keratinocytes through the ERK/Elk-1/Egr-1 signaling pathway. Life Sci. 223, 47–53.
Yi, J., Liu, C., 2010. Molecular characterization of porcine circovirus 2 isolated from diseased pigs co-infected with porcine reproductive and respiratory syndrome virus. Virol. J. 7, 1–4.
Yu, J., Wu, J., Zhang, Y., Guo, L., Cong, X., Du, Y., Li, J., Sun, W., Shi, J., Peng, J., 2012. Concurrent highly pathogenic porcine reproductive and respiratory syndrome virus infection accelerates Haemophilus parasuis infection in conventional pigs. Vet. Microbiol. 158 (3–4), 316–321.
Zhang, Y., Sun, R., Geng, S., Shan, Y., Li, X., Fang, W., 2019. Porcine circovirus type 2 induces ORF3-independent mitochondrial apoptosis via PERK Activation and elevation of cytosolic calcium. J. Virol. 93 (7).
Zhou, Y., Zhou, B., Pache, L., Chang, M., Khodabakhshi, A.H., Tanaseichuk, O., Benner, C., Chanda, S.K., 2019. Metascape provides a biologist-oriented resource for the analysis of systems-level datasets. Nat. Commun. 10 (1), 1–10.
Zhu, Z., Liu, P., Yuan, L., Lian, Z., Hu, D., Yao, X., Li, X., 2021. Induction of UPR promotes interferon response to inhibit PRRSV replication via PKR and NF-κB pathway. Front. Microbiol. 2995.